

Supporting Information for

Green Mechanochemical Synthesis of Imine-Linked Covalent Organic Frameworks for High Iodine Capture

Normanda Brown,¹ Ziad Alsudairy,¹ Ranjan Behera,² Fazli Akram,¹ Kuangcai Chen,³ Kayla Smith-Petty,¹ Bria Motley,¹ Spirit Williams,¹ Wenyu Huang,² Conrad Ingram,¹ Xinle Li^{1*}

¹Department of Chemistry, Clark Atlanta University, Atlanta, Georgia 30314, United States

²Department of Chemistry, Iowa State University, Ames, Iowa 50011, United States

³Imaging Core Facility and Department of Chemistry, Georgia State University, Atlanta, Georgia 30303, United States

Materials and Methods

Reagents

Reagents were obtained from different commercial sources and used as received. 2,5-Dimethoxylbenzene-1,4-dicarboxaldehyde (DMTP, 97%), tris(4-formylphenyl) amine (97%), glacial acetic acid, mesitylene, and 1,4-dioxane were purchased from Sigma Aldrich. Tetrahydrofuran (THF), acetone, and tris(4-aminophenyl) amine (97%) were purchased from Fisher Scientific. 1,3,5-triformylbenzene (TFB, 99.6%), 4,4',4''-(1,3,5,-triazine-2,4,6-triyl) trianiline (TTA, 99.9%), 2,4,6-tris(4-formylphenyl)-1,3,5-triazine (TTB, >98%), and 1,3,5,-tris(4-aminophenyl)benzene (TPB, 99.6%) were purchased from ChemScene. 2,5-dimethyl-1,4-phenylenediamine (PD-CH₃, >98%) was purchased from TCI America. o-Tolidine (95%, pract) was purchased from Acros Organics. *n*-butanol was purchased from Alfa Aesar. 1,2-Dichlorobenzene (99%) and acetonitrile (ACS 99%) were purchased from Thermo Scientific.

Instrumentation

Infrared spectroscopy: Fourier transform infrared (FTIR) spectra were acquired on a Perkin Elmer Spectrum One FT-IR system.

Powder X-ray diffraction (PXRD): PXRD data were collected on a Rigaku MiniFlex 600 X-ray diffractometer with Cu K α 1 radiation ($\lambda = 1.5406 \text{ \AA}$) at 40 kV and 15 mA from $2\theta = 2^\circ$ to 30° with 0.02° increment.

Gas sorption measurements: Nitrogen sorption isotherms were measured on a Micromeritics 3Flex ASAP2020 gas sorption analyzer at 77 K. Before measurement, the COF samples were degassed under vacuum at 120 °C overnight. The specific surface areas were calculated using the Brunauer-Emmett-Teller (BET) method.

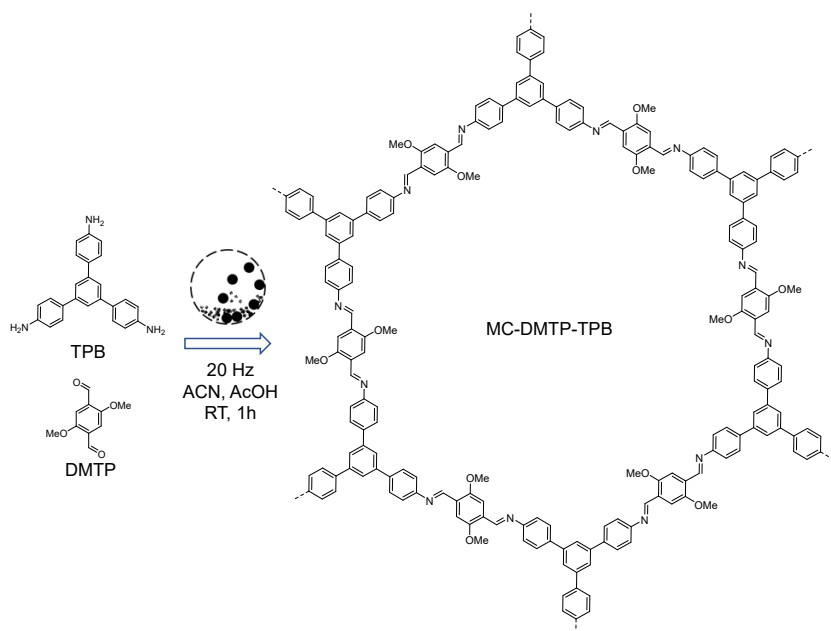
X-ray photoelectron spectroscopy (XPS): XPS measurements were conducted on a Thermo Scientific K-Alpha XPS apparatus equipped with a monochromatic Al K(alpha) source and flood gun for charge compensation.

Thermogravimetric analysis: Thermogravimetric analysis was performed on a TA Instruments Q5000 TGA under N₂ flow (25 mL/min) at a heating rate of 10 °C min⁻¹ up to 900 °C.

Scanning electron microscopy (SEM): SEM images were obtained with a Zeiss Gemini Ultra-55 Analytical Field Emission Scanning Electron Microscope operated at 10 kV using an in-lens detector. Some SEM images (Figures S8-S11) were obtained on a TESCAN Vega 3 scanning electron microscope equipped with a Tungsten electron source and operated at 10 kV using a secondary electron detector. COF samples were sputtered with Au before imaging.

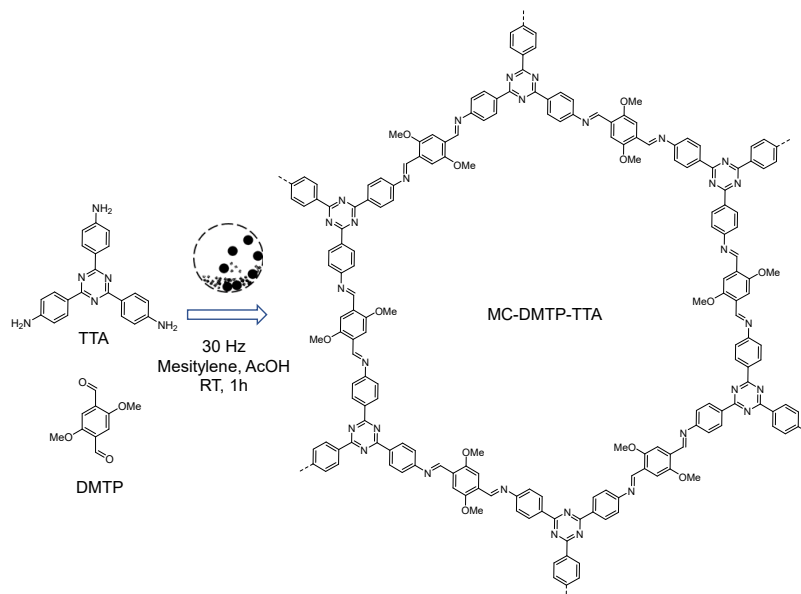
Synthetic Procedures

Mechanochemical synthesis of MC-DMTP-TPB COF



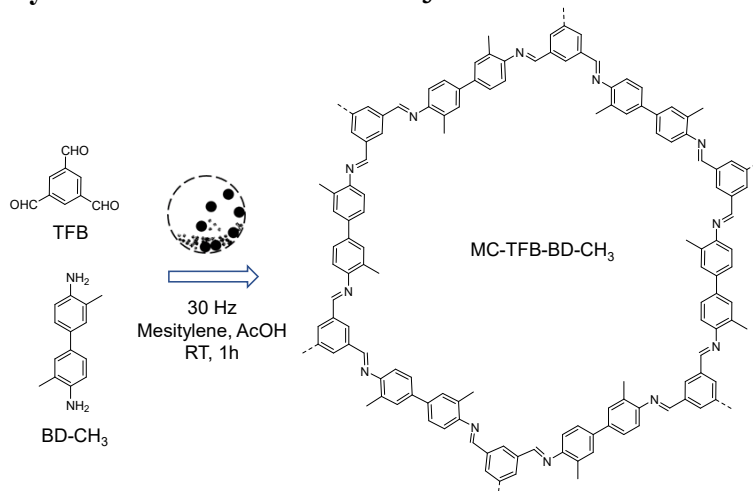
In a 5 mL stainless steel milling jar, 2,5-Dimethoxybenzene-1,4-dicarboxaldehyde (DMTP) (20.4 mg, 0.105 mmol), 1,3,5-tris(4-aminophenyl)benzene (TPB) (24.6 mg, 0.07 mmol), acetonitrile (30 μ L), and glacial acetic acid (15 μ L) were added along with a 5 mm steel ball. The reaction mixture was milled in a Retsch MM 400 Mixer Mill at 20 Hz for 1 hour. The resultant solid was collected via vacuum filtration, washed with THF and acetone, and subjected to Soxhlet extraction using THF as the solvent for 1 day. The collected powder was dried at 120 $^{\circ}$ C under vacuum overnight to give MC-DMTP-TPB in an isolated yield of 98%.

Mechanochemical synthesis of MC-DMTP-TTA COF



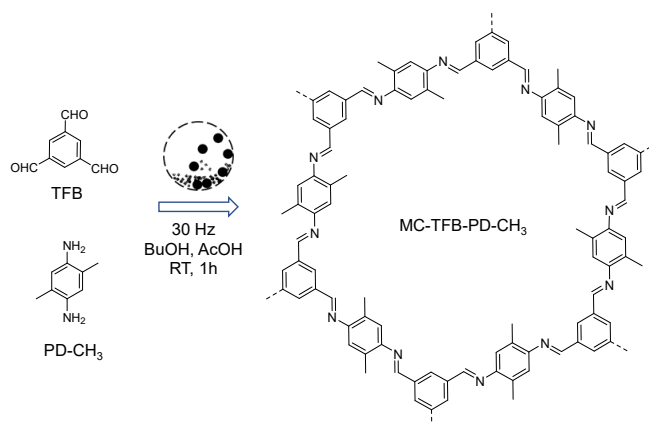
In a 5 mL stainless steel jar, DMTP (20.4 mg, 0.105 mmol), 4,4',4''-(1,3,5-triazine-2,4,6-triyl)trianiline (TTA) (24.8 mg, 0.07 mmol), mesitylene (20 μ L), and glacial acetic acid (20 μ L) were added along with a 5 mm steel ball. The reaction mixture was then milled using Retsch MM 400 Mixer Mill at 30 Hz for 1 hour. The solid was collected via vacuum filtration, washed with THF and acetone, and subjected to Soxhlet extraction using THF for 1 day. The collected powder was dried at 120 $^{\circ}$ C under vacuum overnight to give MC-DMTP-TTA in an isolated yield of 91%.

Mechanochemical synthesis of MC-TFB-BD-CH₃



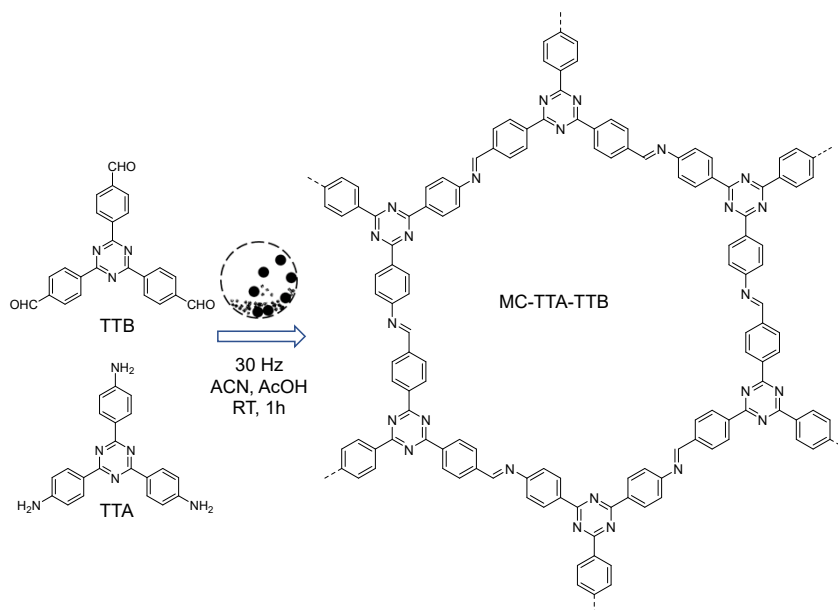
In a 5 mL stainless steel jar, 1,3,5-triformylbenzene (TFB) (11.3 mg, 0.07 mmol), o-tolidine (BD-CH₃, 22.3 mg, 0.105 mmol), mesitylene (15 μ L), and glacial acetic acid (15 μ L) were added along with a 5 mm steel ball. The reaction mixture was then milled using Retsch MM 400 Mixer Mill at 30 Hz for 1 hour. The solid was collected via vacuum filtration, washed with THF and acetone, and subjected to Soxhlet extraction using THF as the solvent for 1 day. The collected powder was dried at 120 $^{\circ}$ C under vacuum overnight, resulting in MC-TFB-BD-CH₃ in an isolated yield of 87%.

Mechanochemical synthesis of MC-TFB-PD-CH₃



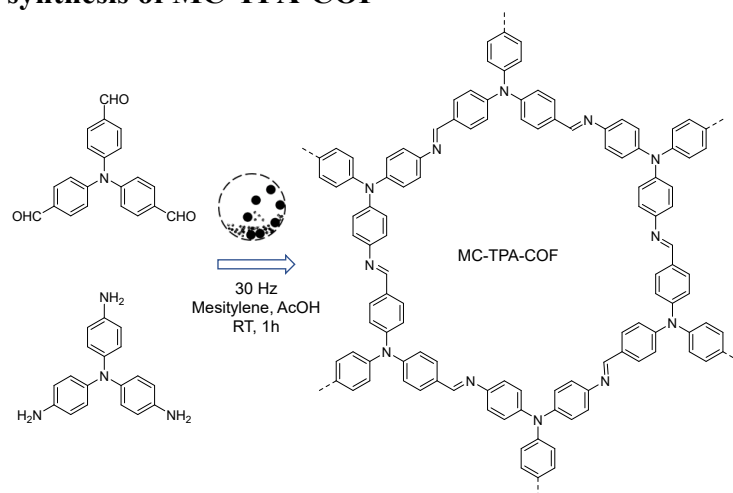
In a 5 mL stainless steel jar, TFB (22.6 mg, 0.14 mmol), 2,5-dimethyl-1,4-phenylenediamine (PD-CH₃) (28.6 mg, 0.21 mmol), *n*-butanol (15 μ L), and glacial acetic acid (20 μ L) were added along with a 5 mm steel ball. The reaction mixture was then milled in a Retsch MM 400 Mixer Mill at 30 Hz for 1 hour. The resulting solid was collected through vacuum filtration, washed with THF and acetone, and subjected to Soxhlet extraction using THF as the solvent for 1 day. The collected powder was dried at 120 $^{\circ}$ C under vacuum overnight to get MC-TFB-PD-CH₃ in an isolated yield of 85%.

Mechanochemical synthesis of MC-TTA-TTB COF



In a 5 mL stainless steel jar, TTA (24.9 mg, 0.07 mmol), 2,4,6-tris(4-formylphenyl)-1,3,5-triazine (TTB) (27.5 mg, 0.07 mmol), acetonitrile (15 μ L), and glacial acetic acid (20 μ L) were added with a 5 mm steel ball. The reaction mixture was milled in a Retsch MM 400 Mixer Mill at 30 Hz for 1 hour. The solid was collected via vacuum filtration, washed with THF and acetone followed by Soxhlet extraction using THF as the solvent for 1 day. The powder collected was dried at 120 $^{\circ}$ C under vacuum overnight to get MC-TTA-TTB COF in an isolated yield of 91%.

Mechanochemical synthesis of MC-TPA-COF



In a 5 mL stainless steel jar, tris(4-formylphenyl) amine (20.3 mg, 0.07 mmol), tris(4-aminophenyl) amine (23.1 mg, 0.07 mmol), mesitylene (20 μ L), and glacial acetic acid (20 μ L) were added along with a 5 mm steel ball. The reaction mixture was milled in a Retsch MM 400 Mixer Mill at 30 Hz for 1 hour. The solid was collected via vacuum filtration, washed with THF and acetone followed by Soxhlet extraction using THF as the solvent for 1 day. The powder collected was dried at 120 $^{\circ}$ C under vacuum overnight to get MC-TPA-COF in an isolated yield of 86%.

Conventional solvothermal synthesis of DMTP-TPB COF

This COF was synthesized based on a reported procedure.¹ In a 5 mL Biotage microwave vial, DMTP (46 mg, 0.24 mmol) and TPB (56 mg, 0.16 mmol) were dissolved by sonication in a mixture of 1,2-dichlorobenzene/*n*-butanol (1 mL/1 mL). Next, 6 M aqueous acetic acid (0.2 mL) was added to the mixture. The vial was sealed, subjected to three cycles of freeze-pump-thaw process, and then heated under vacuum in an oven at 120 $^{\circ}$ C for 3 days. The resulting precipitates were collected by vacuum filtration, subjected to Soxhlet extraction using THF as the solvent for 1 day, and dried at 120 $^{\circ}$ C under vacuum overnight to give a yellow powder in ~90 % yield.

Static iodine vapor adsorption

An open glass vial (1 mL) containing activated COFs (~25 mg) was placed inside a Scintillation vial (20 mL), which contains iodine solids (2 g). The Scintillation vial was sealed and kept at 75 $^{\circ}$ C in an oven. After a certain period of exposure time, the Scintillation vial was removed from the oven and allowed to room temperature. The small vial containing COFs was weighted and placed back into the Scintillation vial. The Scintillation vial was resealed and returned to the oven to continue the iodine adsorption until the weight of the small vial containing COFs remained constant. The static iodine adsorption capacity of the COF was determined using the following equation:

$$Q = (W_f - W_i)/W_i$$

Where:

Q (g g⁻¹) refers to the adsorption capacity

W_f = final weight of COF after the adsorption of iodine

W_i = initial weight of COF before the adsorption of iodine

Recycling the COF adsorbent through thermal desorption

The iodine-captured MC-DMTP-TPB COF sample was placed in a vacuum oven at 135 °C overnight. The successful removal of adsorbed iodine from the COF was confirmed by the apparent changes in both weight and color of the sample. The regenerated COF was subjected to the next cycle.

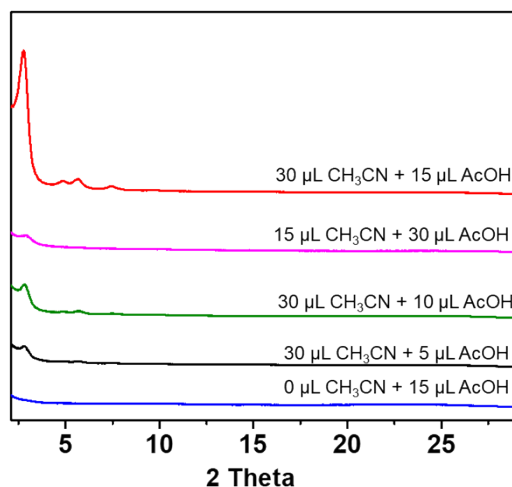


Figure S1. The effect of catalyst and LAG additive amount on the crystallinity of MC-DMTP-TPB COF, which was made by milling DMTP (20.4 mg, 0.105 mmol) with TPB (24.6 mg, 0.07 mmol) at 20 Hz for 1 hour using glacial acetic acid and acetonitrile as the LAG additive.

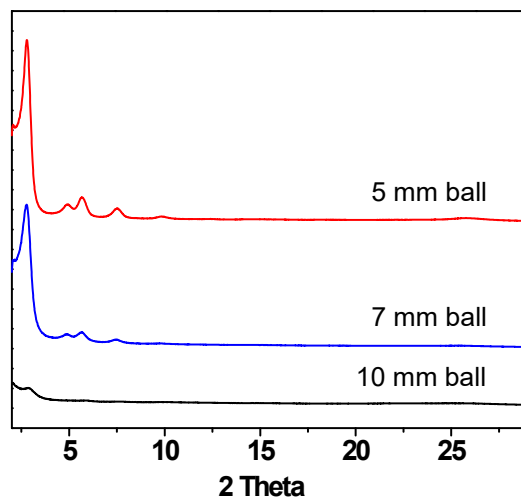


Figure S2. The effect of grinding ball size on the crystallinity of MC-DMTP-TPB COF, which was made by milling DMTP (20.4 mg, 0.105 mmol) with TPB (24.6 mg, 0.07 mmol) at 20 Hz for 1 hour using glacial acetic acid (15 μL) and acetonitrile (30 μL) as the LAG additive.

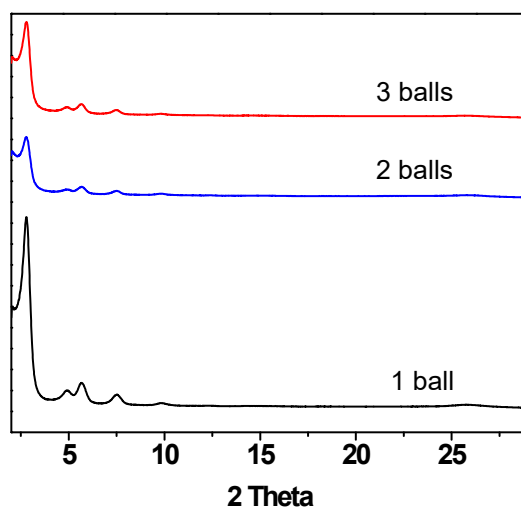


Figure S3. The effect of the number of the ball (5 mm in diameter) on the crystallinity of MC-DMTP-TPB COF, which was made by milling DMTP (20.4 mg, 0.105 mmol) with TPB (24.6 mg, 0.07 mmol) at 20 Hz for 1 hour using glacial acetic acid (15 μ L) and acetonitrile (30 μ L) as the LAG additive.

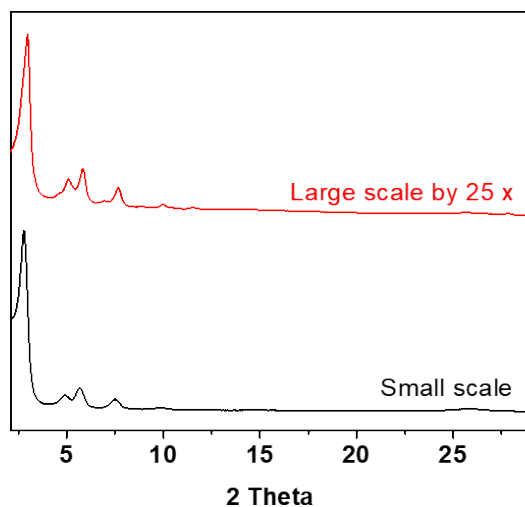


Figure S4. Scalable synthesis of MC-DMTP-TPB COF, which was made by milling DMTP (510 mg, 2.625 mmol) with TPB (615 mg, 1.75 mmol) at 20 Hz for 1 hour using a 10-mm diameter stainless steel ball in the presence of glacial acetic acid (375 μ L) and acetonitrile (750 μ L). Inset digital photo shows the large-scale production of COF (0.8647g).

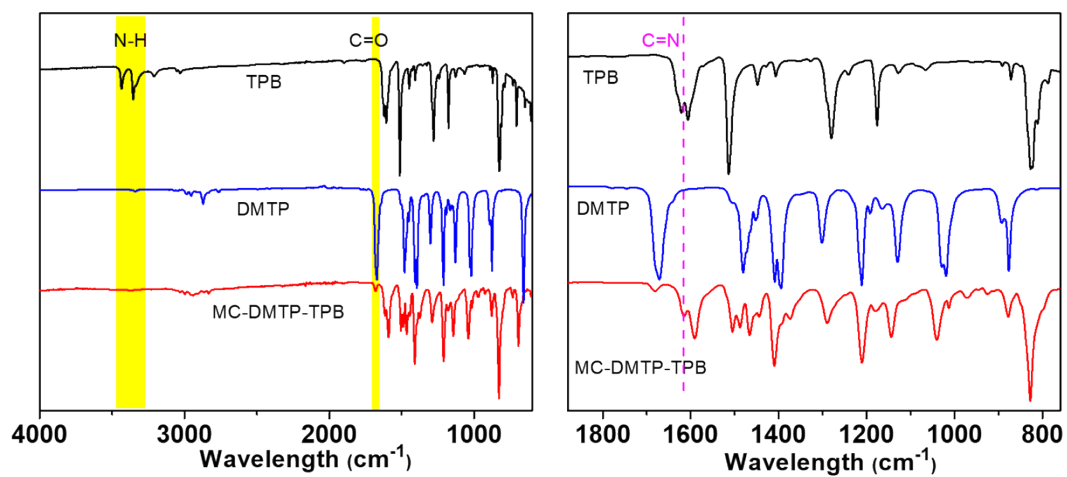


Figure S5. FTIR spectra of MC-DMTP-TPB COF and its monomers, TPB and DMTP.

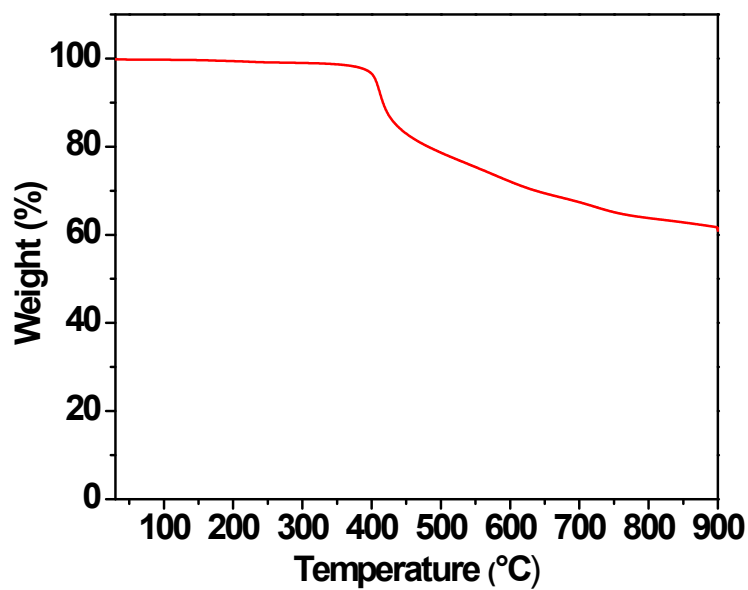


Figure S6. TGA curve of MC-DMTP-TPB COF under an N_2 atmosphere.

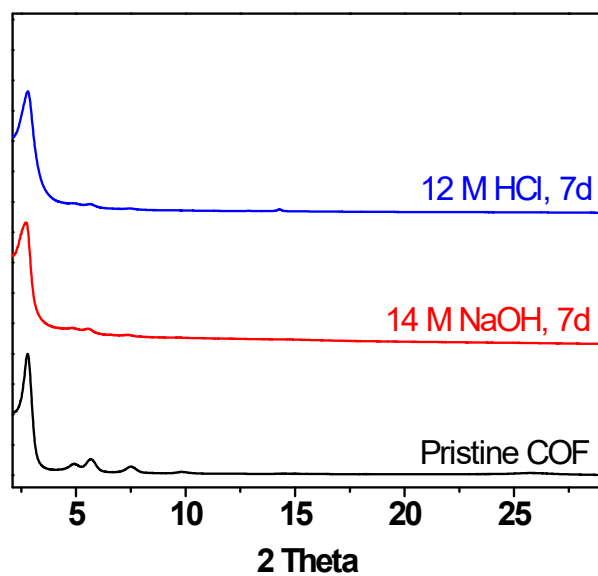


Figure S7. PXRD patterns of MC-DMTP-TPB COF after being exposed to 12 M HCl and 14 M NaOH aqueous solution for 7 days.

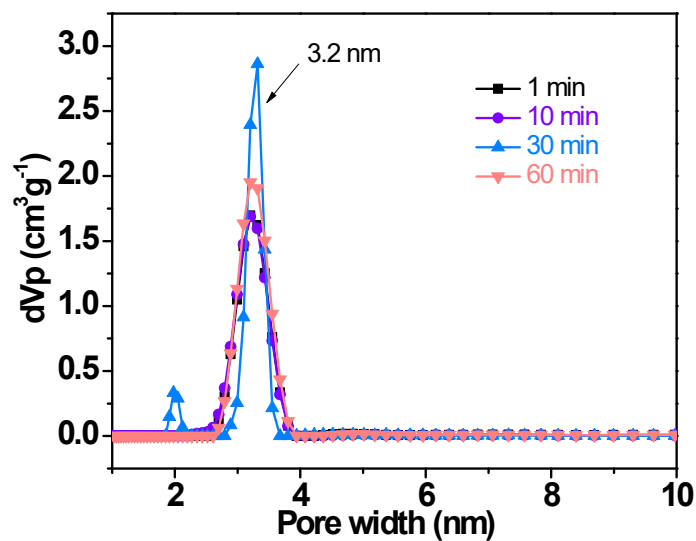


Figure S8. Pore size distribution profiles of MC-DMTP-TPB at different milling times, which were obtained by fitting the N_2 sorption isotherms using a quenched solid-state density functional theory (QSDFT) model.

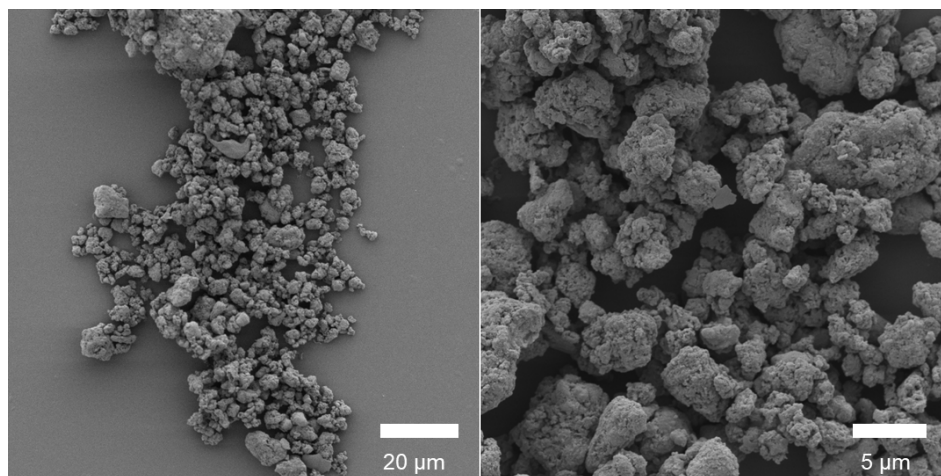


Figure S9. SEM images of MC-DMTP-TPB COF (1 h) at different magnifications.

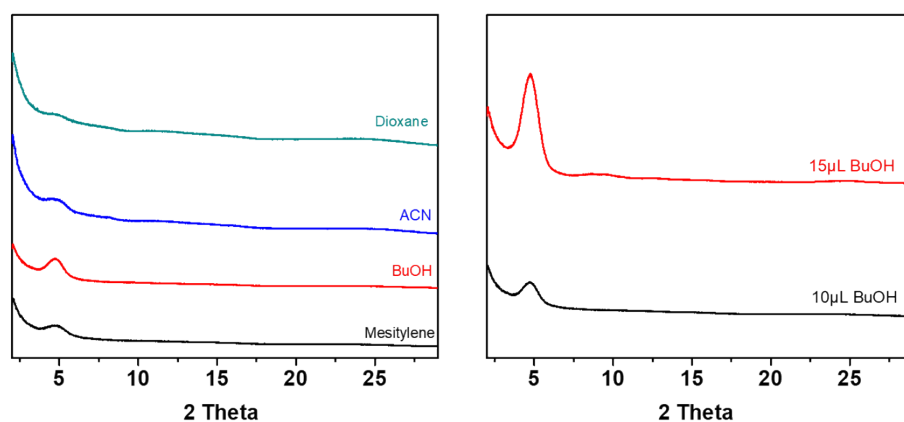


Figure S10. Condition screening for MC-TFB-PD-CH₃, which was made by milling 1,3,5-triformylbenzene (TFB) and 2,5-dimethyl-1,4-phenylenediamine (PD-CH₃) at 30 Hz for 1 hour using various LAG additives and glacial acetic acid with one 5 mm diameter stainless steel ball per jar.

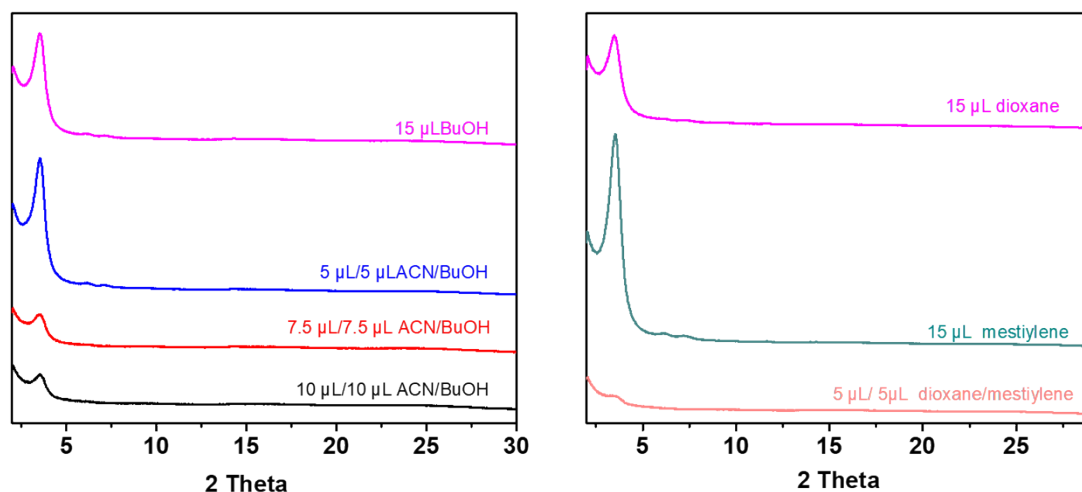


Figure S11. Condition screening for MC-TFB-BD-CH₃, which was constructed by milling 1,3,5-triformylbenzene (TFB) (11.3 mg, 0.07 mmol) and o-tolidine (22.3 mg, 0.105 mmol) at 30 Hz for 1 h using various LAG additive and glacial acetic acid (15 μ L) with a 5 mm diameter stainless steel ball per jar.

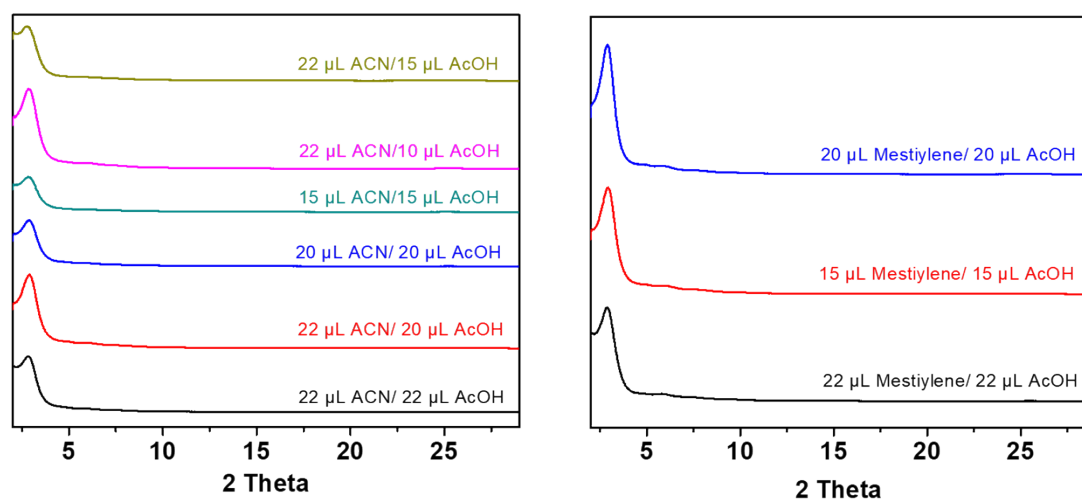


Figure S12. Condition screening for MC-DMTP-TTA, which was made by milling DMTP (20.4 mg, 0.105 mmol) and TTA (24.8 mg, 0.07 mmol) at 30 Hz for 1 hour using various LAG additives and glacial acetic acid with one 5 mm diameter stainless steel ball per jar.

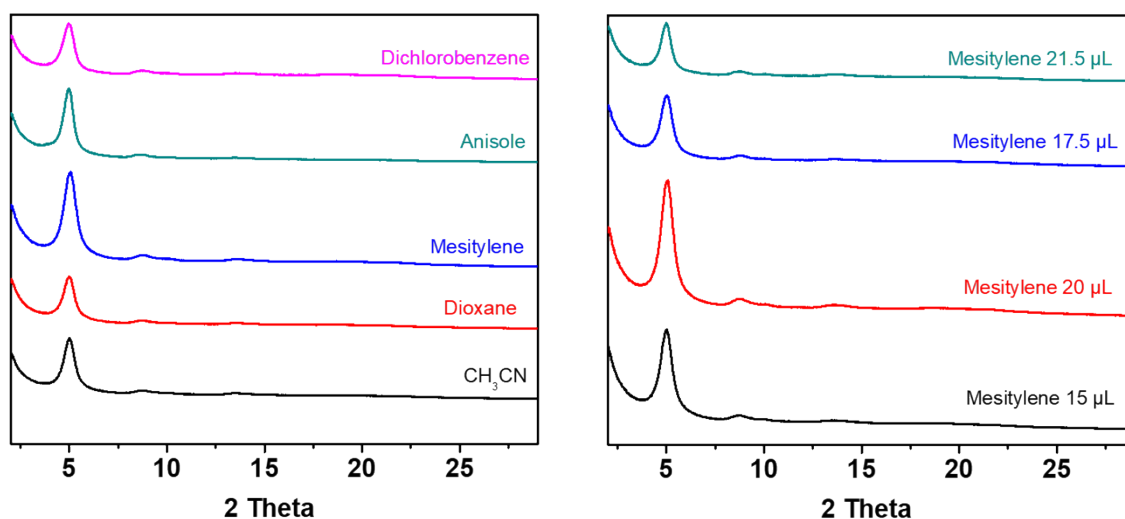


Figure S13. Condition screening for MC-TPA COF, which was made by milling tris(4-formylphenyl) amine and tris(4-aminophenyl) amine at 30 Hz for 1 hour using various LAG additives and glacial acetic acid with one 5 mm diameter stainless steel ball per jar.

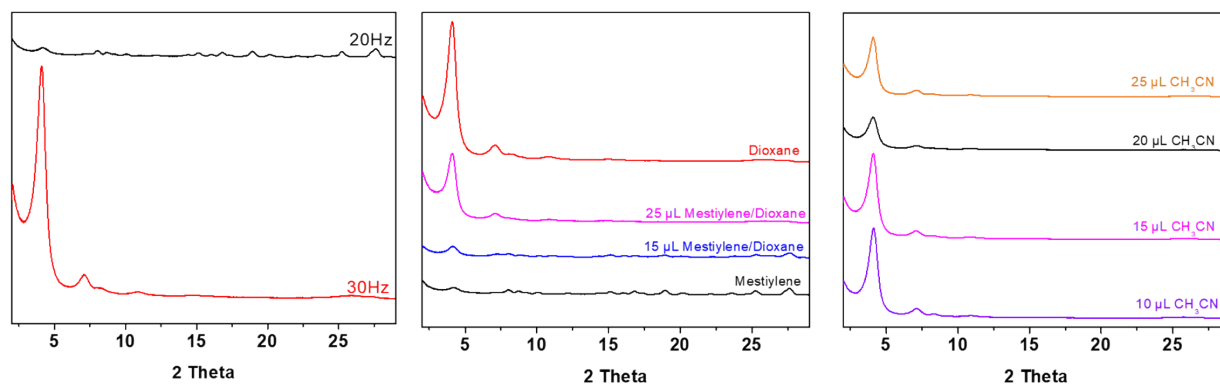


Figure S14. Condition screening for MC-TTA-TTB COF, which was made by milling TTA and TTb for 1 hour using various LAG additives and glacial acetic acid with one 5 mm diameter stainless steel ball.

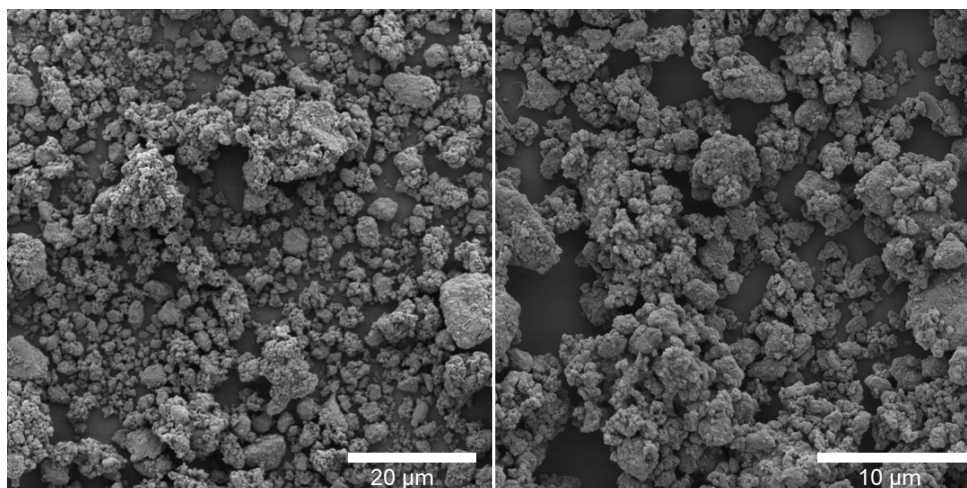


Figure S15. SEM images of MC-DMTP-TTA COF at different magnifications.

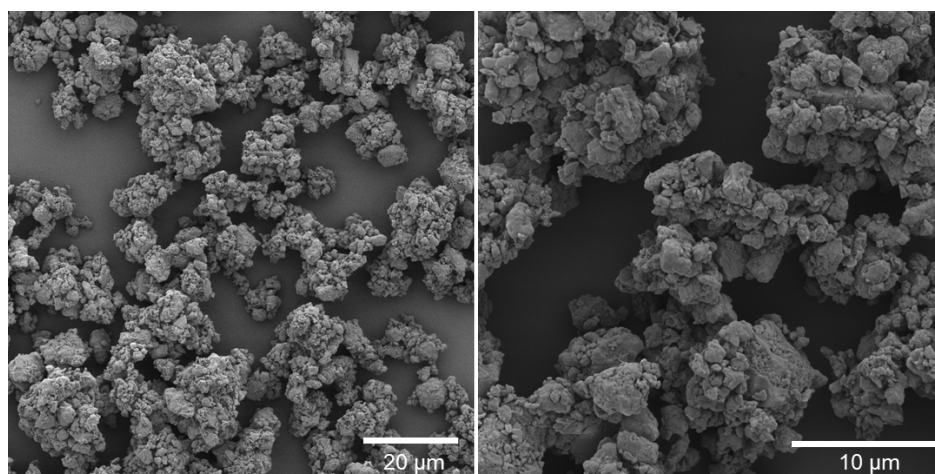


Figure S16. SEM images of MC-TFB-BD-CH₃ COF at different magnifications.

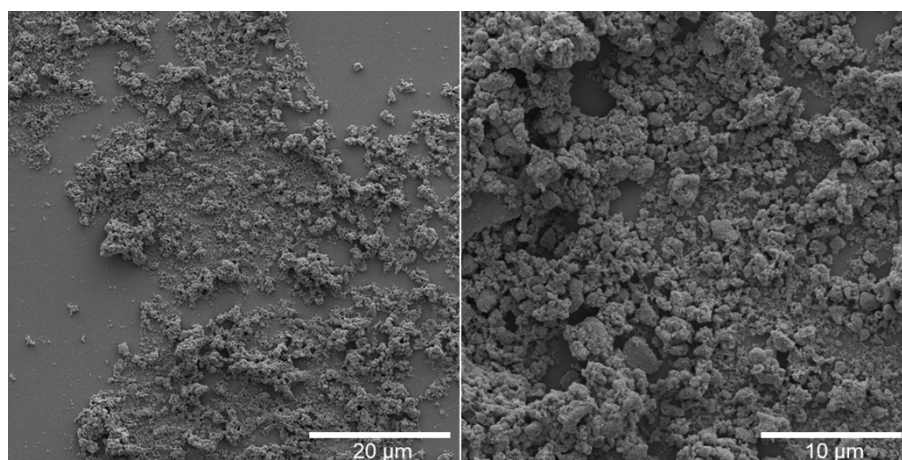


Figure S17. SEM images of MC-TFB-PD-CH₃ COF at different magnifications.

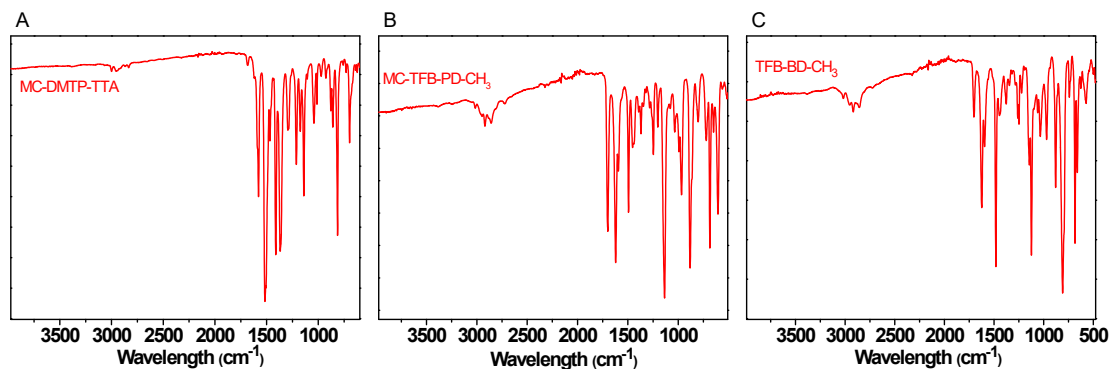


Figure S18. FTIR spectra of (A) MC-DMTP-TTA, (B) MC-TFB-BD-CH₃, and (C) MC-TFB-PD-CH₃.

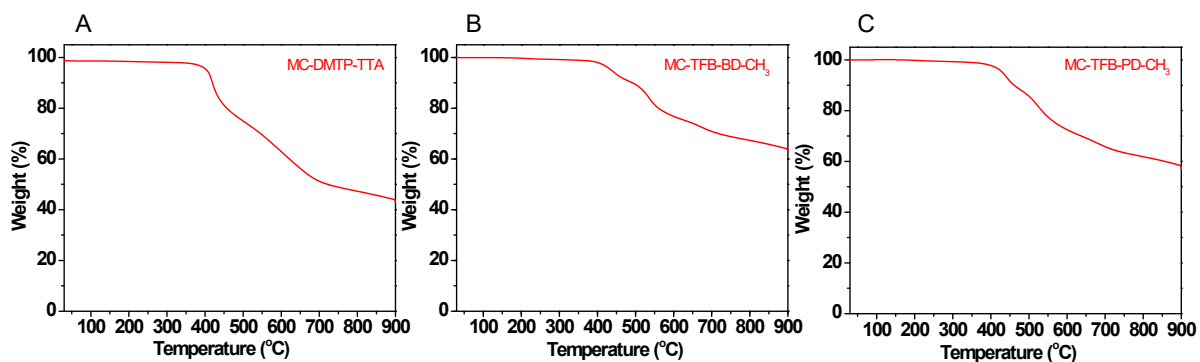


Figure S19. TGA curves of (A) MC-DMTP-TTA, (B) MC-TFB-BD-CH₃, and (C) MC-TFB-PD-CH₃ COFs under an N₂ atmosphere.

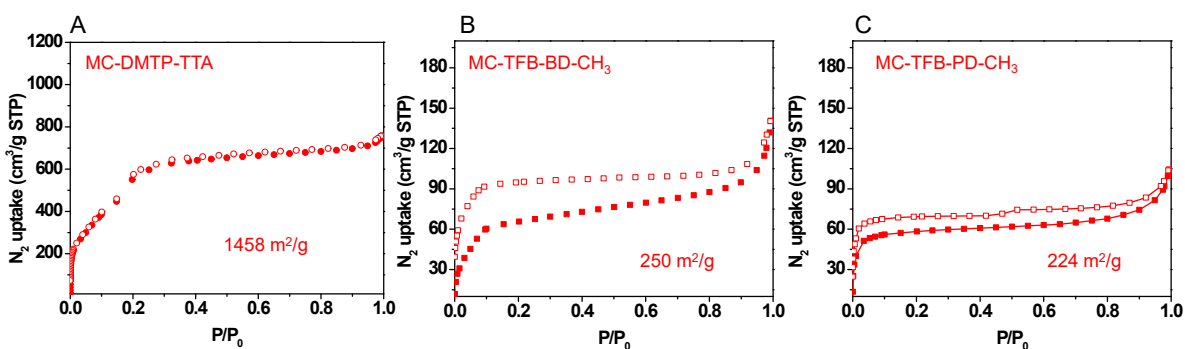


Figure S20. N₂ sorption isotherms of (A) MC-DMTP-TTA, (B) MC-TFB-BD-CH₃, and (C) MC-TFB-PD-CH₃ COFs.

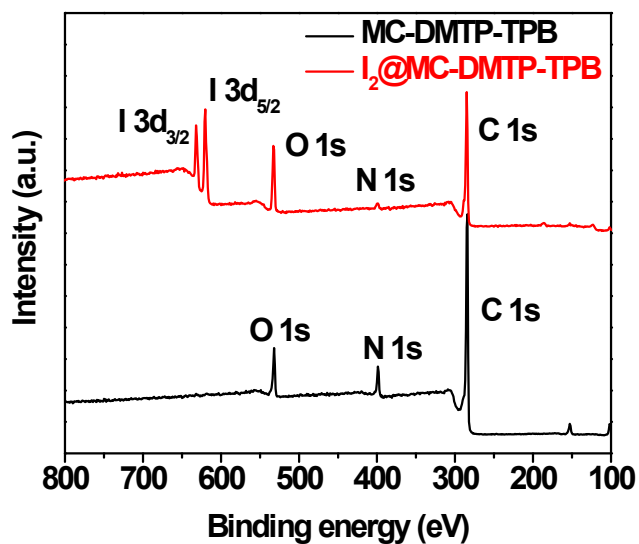


Figure S21. XPS survey spectra of MC-DMTP-TPB before and after iodine capture.

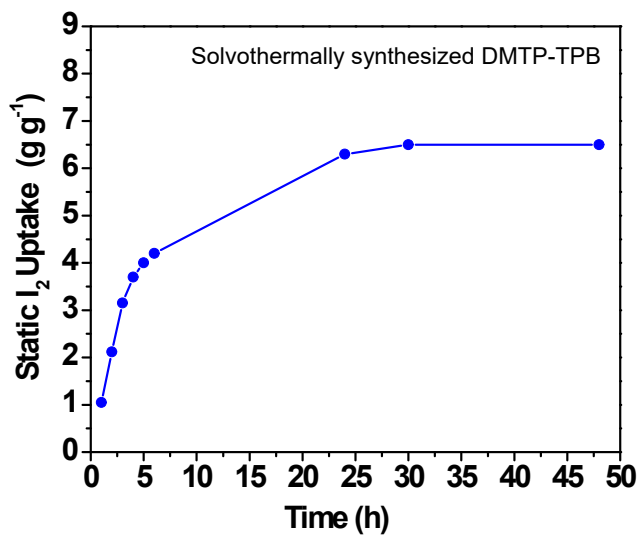


Figure S22. The gravimetric iodine adsorption capacity of solvothermally synthesized DMTP-TPB COF as a function of exposure time at 75 °C and ambient pressure. DMTP-TPB COF showed an iodine adsorption capacity of 6.4 g g⁻¹, which is consistent with the previous report.²

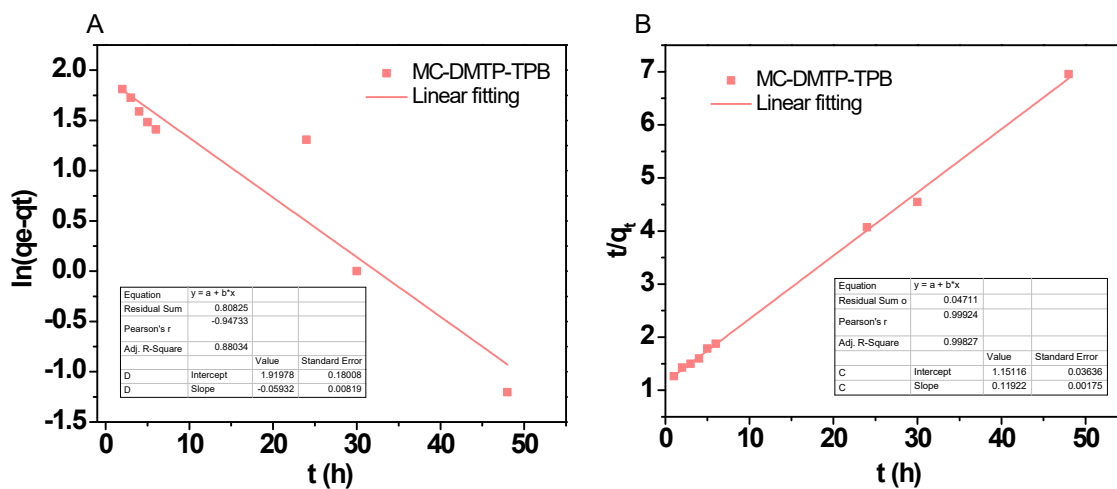


Figure S23. The fitting curves for (A) pseudo-first-order and (B) pseudo-second-order kinetic model of iodine adsorption on MC-DMTP-TPB COF.

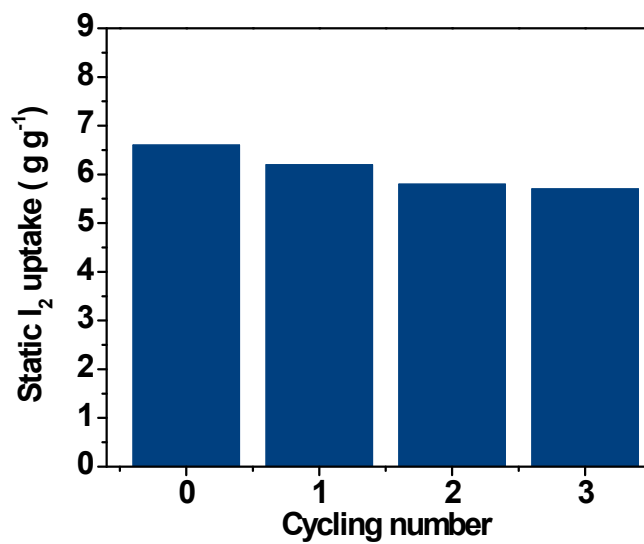


Figure S24. The recycling test of MC-DMTP-TPB COF in three successive adsorption-desorption cycles at 75 °C.

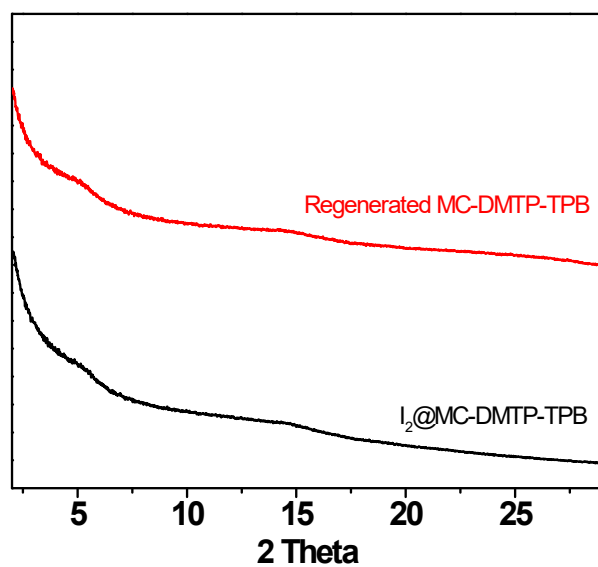


Figure S25. PXRD patterns of I₂@MC-DMTP-TPB (black curve) and regenerated MC-DMTP-TPB COF (red curve).

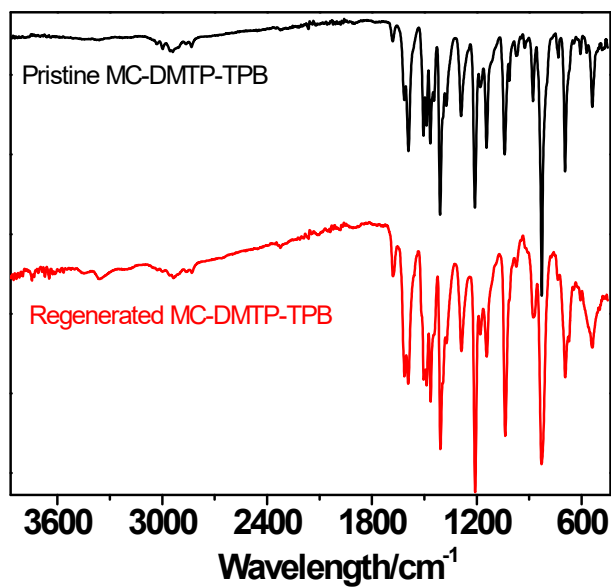


Figure S26. FTIR spectra of pristine MC-DMTP-TPB COF (black curve) and regenerated MC-DMTP-TPB COF (red curve).

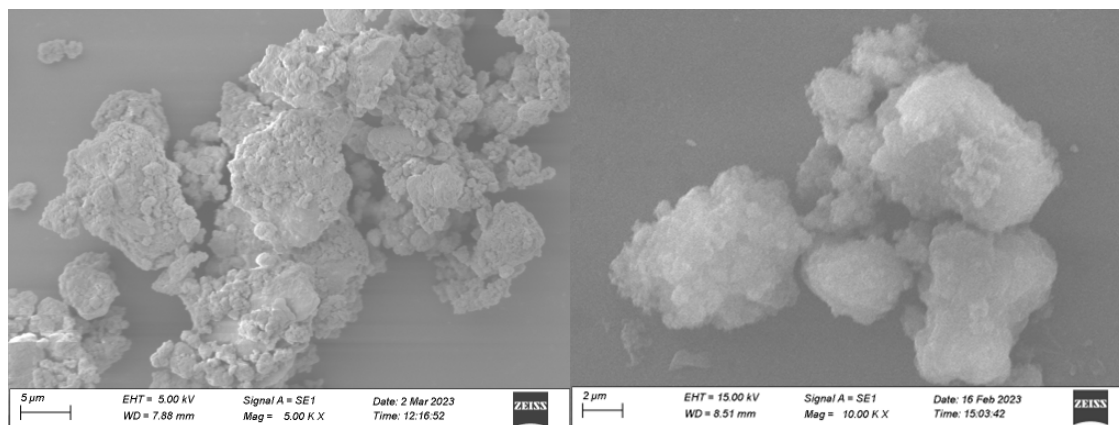


Figure S27. SEM images of regenerated MC-DMTP-TPB COF at different magnifications.

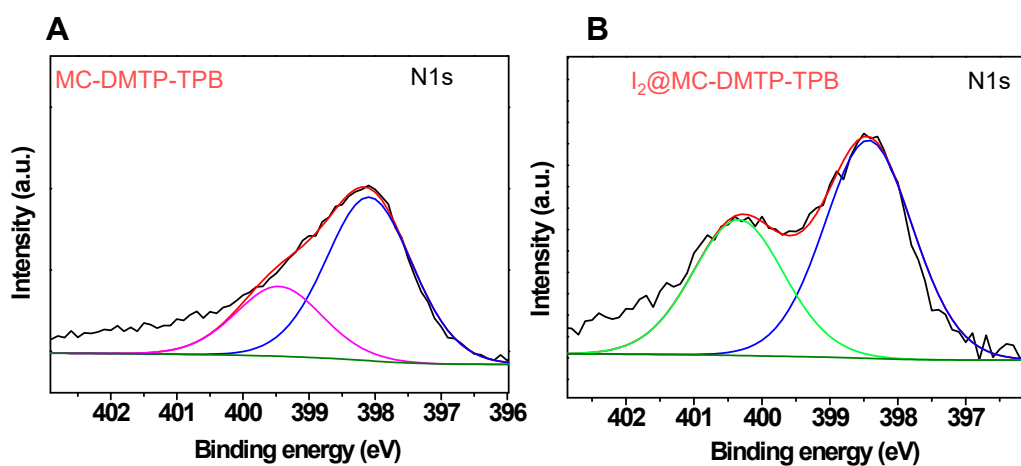


Figure S28. N 1s XPS spectra of (A) pristine MC-DMTP-TPB and (B) $I_2@MC-DMTP-TPB$. Note: The N1s peak centered at 399.5 eV is assigned to the unreacted $-NH_2$ at the defective edges of COF.

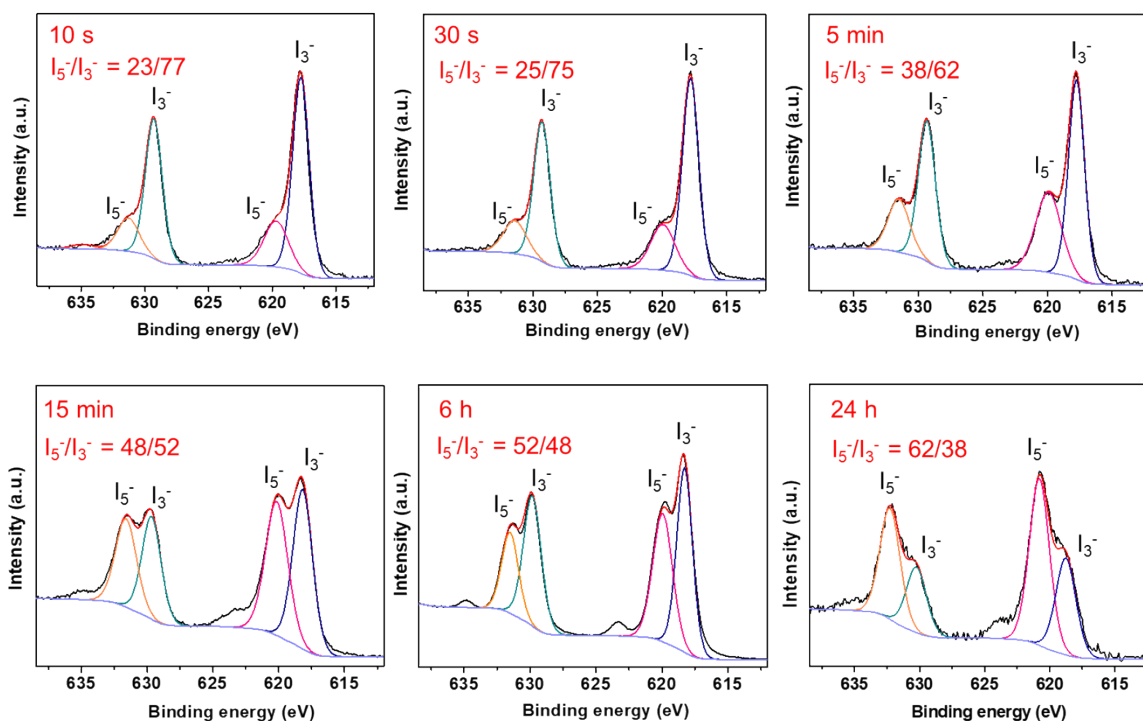


Figure S29. I3d XPS spectra of I₂@MC-DMTP-TPB after different exposure times of iodine vapor.

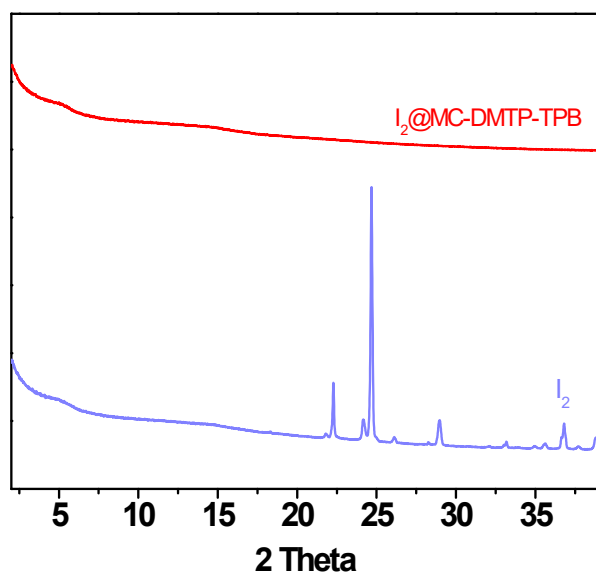


Figure S30. PXRD patterns of molecular iodine (blue curve) and I₂@MC-DMTP-TPB (red curve).

Table S1. Summary of reported COFs made rapidly (< 1 h) at ambient temperature.

Entry	COFs	Temperature	Condition	Time	S _{BET} (m ² g ⁻¹)	Activation	Reference
1	MC-DMTP-TPB	RT	Air, ball mill nearly solventless AcOH	1 min	1387	Vacuum activation	This work
				10 min	1400		
				30 min	1517		
				60 min	1554		
2	TpBa series	RT Then 170 °C	Air, ball mill <i>p</i> -toluenesulfonic acid	1 min then 1 h	538- 3109	Vacuum activation	3
3	TAPB-PDA	20 °C	Air Mesitylene/dioxane Sc(OTf) ₃	10 min	2175	Supercritical CO ₂ activation	4
4	sonoCOF-1	RT	Air, ultrasound 6 M AcOH	60 min	2059	Vacuum activation	5
5	UV-COF-5	RT	Air, UV Mesitylene/dioxane	60 min	2026	Vacuum activation	6
6	JUC-523	RT	Air, H ₂ O AcOH	30 min	1435	Vacuum activation	7
7	TpBD	RT	Air, EtOH AcOH	30 min	885	Vacuum activation	8
8	EB-COF-1	RT	N ₂ , 100 kGy 2-dichlorobenzene/ <i>n</i> - butanol 6 M AcOH	160 s	738	Vacuum activation	9
9	COF-42-B	RT	Air Mesitylene/dioxane Sc(OTf) ₃	30 min	367	Vacuum activation	10
10	RT-COF-1	RT	Air, DMSO AcOH	1 min	329	Vacuum activation	11
11	TpPa-1 (MC)	RT	Air, solventless grinding	40 min	61	Vacuum activation	12

Table S2. Summary of static iodine vapor capture capacities and synthetic conditions of high-performing COF adsorbents.

Entry	COF adsorbents	Temperature (°C)	S _{BET} (m ² g ⁻¹)	I ₂ uptake (g g ⁻¹)	Synthetic condition	Reference
1	MC-DMTP-TPB	75	1554	6.9	RT, 1 h, ball mill Air, nearly solventless	This work
	MC-DMTP-TTA		1458	7.1		
	MC-TPB-BD-CH ₃		250	6.5		
	MC-TPB-PD-CH ₃		223	6.4		
2	iCOF-AB-50	75	1390	10.21	1. 120 °C, 3 d, vacuum 2. PSM, 140 °C, 3 d	13
3	iCOF-AB-33	75	1580	9.00		
4	COF-TAPT	75	2348	8.61	120 °C, 3 d, vacuum	14
5	JUC-561	75	2359	8.19	120 °C, 3 d, vacuum	15
6	COFA-1 aerogel	75	254.6	8.15	RT, 1 d, freeze-dry	16
7	COF-TAPB	75	2290	7.94	120 °C, 3 d, vacuum	14
8	Mw-TPB-BD-CH ₃	75	210	7.83	90 °C, 1 h microwave, air	17
9	TAPB-PDA aerogel	75	2273	7.7	80 °C, 12 h ScCO ₂ activation	18
10	COF-AB-33	75	2172	6.81	120 °C, 3 d, vacuum	13
11	COF-AB-50	75	2103	6.49		
12	QTD-COF-V	75	/	6.29	1. PSM, RT, 2 d 2. 120 °C, 7 d	19
13	DMTP-TPB	77	1927	6.26	120 °C, 3 d, vacuum	2
14	C-TP-BPDA-COF	75	436	6.11	120 °C, 3 d, vacuum	20
15	SCU-COF-2	75	413.4	6.0	120 °C, 3 d, vacuum	21
16	PB-TT COF	75	1305.3	5.97	120 °C, 3 d, vacuum	22
17	JUC-609	75	1012.81	5.90	120 °C, 3 d, vacuum	23
18	USTB-1c	75	1454	5.80	120 °C, 3 d, vacuum	24
19	TJNU-201	77	2510	5.625	1. PSM, 65 °C, 30 h 2. 120 °C 3 d, vacuum	25

References

1. X. Li, C. Zhang, S. Cai, X. Lei, V. Altoc, F. Hong, J. J. Urban, J. Ciston, E. M. Chan and Y. Liu, Facile transformation of imine covalent organic frameworks into ultrastable crystalline porous aromatic frameworks, *Nat. Commun.*, 2018, **9**, 1-8.
2. P. Wang, Q. Xu, Z. Li, W. Jiang, Q. Jiang and D. Jiang, Exceptional iodine capture in 2D covalent organic frameworks, *Adv. Mater.*, 2018, **30**, 1801991.

3. S. Karak, S. Kandambeth, B. P. Biswal, H. S. Sasmal, S. Kumar, P. Pachfule and R. Banerjee, Constructing Ultraporous Covalent Organic Frameworks in Seconds via an Organic Terracotta Process, *J. Am. Chem. Soc.*, 2017, **139**, 1856-1862.
4. M. Matsumoto, R. R. Dasari, W. Ji, C. H. Feriante, T. C. Parker, S. R. Marder and W. R. Dichtel, Rapid, Low Temperature Formation of Imine-Linked Covalent Organic Frameworks Catalyzed by Metal Triflates, *J. Am. Chem. Soc.*, 2017, **139**, 4999-5002.
5. W. Zhao, P. Yan, H. Yang, M. Bahri, A. M. James, H. Chen, L. Liu, B. Li, Z. Pang, R. Clowes, N. D. Browning, J. W. Ward, Y. Wu and A. I. Cooper, Using sound to synthesize covalent organic frameworks in water, *Nat. Syn.*, 2022, **1**, 87-95.
6. S. Kim, C. Park, M. Lee, I. Song, J. Kim, M. Lee, J. Jung, Y. Kim, H. Lim and H. C. Choi, Rapid Photochemical Synthesis of Sea-Urchin-Shaped Hierarchical Porous COF-5 and Its Lithography-Free Patterned Growth, *Adv. Funct. Mater.*, 2017, **27**, 1700925.
7. Y. Liu, Y. Wang, H. Li, X. Guan, L. Zhu, M. Xue, Y. Yan, V. Valtchev, S. Qiu and Q. Fang, Ambient aqueous-phase synthesis of covalent organic frameworks for degradation of organic pollutants, *Chem. Sci.*, 2019, **10**, 10815-10820.
8. C.-X. Yang, C. Liu, Y.-M. Cao and X.-P. Yan, Facile room-temperature solution-phase synthesis of a spherical covalent organic framework for high-resolution chromatographic separation, *Chem. Commun.*, 2015, **51**, 12254-12257.
9. M. Zhang, J. Chen, S. Zhang, X. Zhou, L. He, M. V. Sheridan, M. Yuan, M. Zhang, L. Chen, X. Dai, F. Ma, J. Wang, J. Hu, G. Wu, X. Kong, R. Zhou, T. E. Albrecht-Schmitt, Z. Chai and S. Wang, Electron Beam Irradiation as a General Approach for the Rapid Synthesis of Covalent Organic Frameworks under Ambient Conditions, *J. Am. Chem. Soc.*, 2020, **142**, 9169-9174.
10. M. Li, S. Qiao, Y. Zheng, Y. H. Andaloussi, X. Li, Z. Zhang, A. Li, P. Cheng, S. Ma and Y. Chen, Fabricating Covalent Organic Framework Capsules with Commodious Microenvironment for Enzymes, *J. Am. Chem. Soc.*, 2020, **142**, 6675-6681.
11. A. de la Peña Ruigómez, D. Rodríguez-San-Miguel, K. C. Stylianou, M. Cavallini, D. Gentili, F. Liscio, S. Milita, O. M. Roscioni, M. L. Ruiz-González and C. Carbonell, Direct On-Surface Patterning of a Crystalline Laminar Covalent Organic Framework Synthesized at Room Temperature, *Eur. J. Chem.*, 2015, **21**, 10666-10670.
12. B. P. Biswal, S. Chandra, S. Kandambeth, B. Lukose, T. Heine and R. Banerjee, Mechanochemical synthesis of chemically stable isorecticular covalent organic frameworks, *J. Am. Chem. Soc.*, 2013, **135**, 5328-5331.
13. Y. Xie, T. Pan, Q. Lei, C. Chen, X. Dong, Y. Yuan, J. Shen, Y. Cai, C. Zhou and I. Pinnau, Ionic Functionalization of Multivariate Covalent Organic Frameworks to Achieve an Exceptionally High Iodine-Capture Capacity, *Angew. Chem. Int. Ed.*, 2021, **60**, 22432-22440.
14. Y. Xie, T. Pan, Q. Lei, C. Chen, X. Dong, Y. Yuan, W. A. Maksoud, L. Zhao, L. Cavallo and I. Pinnau, Efficient and simultaneous capture of iodine and methyl iodide achieved by a covalent organic framework, *Nat. Commun.*, 2022, **13**, 1-10.
15. J. Chang, H. Li, J. Zhao, X. Guan, C. Li, G. Yu, V. Valtchev, Y. Yan, S. Qiu and Q. Fang, Tetrathiafulvalene-based covalent organic frameworks for ultrahigh iodine capture, *Chem. Sci.*, 2021, **12**, 8452-8457.
16. X. Li, Z. Jia, J. Zhang, Y. Zou, B. Jiang, Y. Zhang, K. Shu, N. Liu, Y. Li and L. Ma, Moderate and Universal Synthesis of Undoped Covalent Organic Framework Aerogels for Enhanced Iodine Uptake, *Chem. Mater.*, 2022, **34**, 11062-11071.

17. Z. Alsudairy, N. Brown, C. Yang, S. Cai, F. Akram, A. Ambus, C. Ingram and X. Li, Facile Microwave-Assisted Synthesis of 2D Imine-Linked Covalent Organic Frameworks for Exceptional Iodine Capture, *Precision Chemistry*, 2023, DOI: 10.1021/prechem.3c00006.
18. D. Zhu, Y. Zhu, Q. Yan, M. Barnes, F. Liu, P. Yu, C.-P. Tseng, N. Tjahjono, P.-C. Huang, M. M. Rahman, E. Egap, P. M. Ajayan and R. Verduzco, Pure Crystalline Covalent Organic Framework Aerogels, *Chem. Mater.*, 2021, **33**, 4216-4224.
19. X. Guo, Y. Li, M. Zhang, K. Cao, Y. Tian, Y. Qi, S. Li, K. Li, X. Yu and L. Ma, Colyliform Crystalline 2D Covalent Organic Frameworks (COFs) with Quasi-3D Topologies for Rapid I₂ Adsorption, *Angew. Chem. Int. Ed.*, 2020, **59**, 22697-22705.
20. L. Zhai, S. Sun, P. Chen, Y. Zhang, Q. Sun, Q. Xu, Y. Wu, R. Nie, Z. Li and L. Mi, Constructing cationic covalent organic frameworks by a post-function process for an exceptional iodine capture via electrostatic interactions, *Mater. Chem. Front.*, 2021, **5**, 5463-5470.
21. L. He, L. Chen, X. Dong, S. Zhang, M. Zhang, X. Dai, X. Liu, P. Lin, K. Li and C. Chen, A nitrogen-rich covalent organic framework for simultaneous dynamic capture of iodine and methyl iodide, *Chem*, 2021, **7**, 699-714.
22. X. Yan, Y. Yang, G. Li, J. Zhang, Y. He, R. Wang, Z. Lin and Z. Cai, Thiophene-based covalent organic frameworks for highly efficient iodine capture, *Chin. Chem. Lett.*, 2023, **34**, 107201.
23. J. Zhang, J. Liu, Y. Liu, Y. Wang, Q. Fang and S. Qiu, A Two-dimensional Covalent Organic Framework for Iodine Adsorption, *Chem. Res. Chin. Univ.*, 2022, **38**, 456-460.
24. C. Liu, Y. Jin, Z. Yu, L. Gong, H. Wang, B. Yu, W. Zhang and J. Jiang, Transformation of Porous Organic Cages and Covalent Organic Frameworks with Efficient Iodine Vapor Capture Performance, *J. Am. Chem. Soc.*, 2022, **144**, 12390-12399.
25. J. Li, H. Zhang, L. Zhang, K. Wang, Z. Wang, G. Liu, Y. Zhao and Y. Zeng, Two-dimensional covalent-organic frameworks for ultrahigh iodine capture, *J. Mater. Chem. A.*, 2020, **8**, 9523-9527.